

# Nucleotidyl Cyclase Activity of Soluble Guanylyl Cyclase $\alpha_1\beta_1$

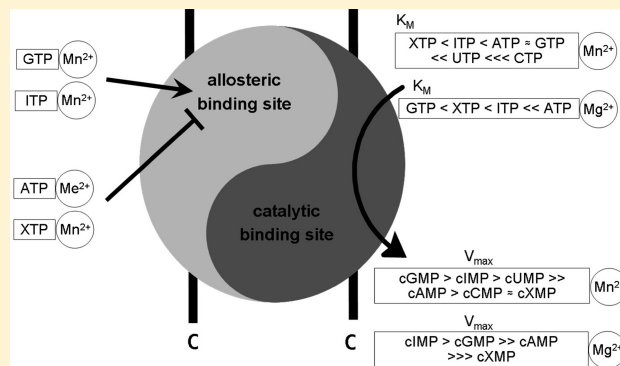
Kerstin Y. Beste,<sup>†</sup> Heike Burhenne,<sup>†</sup> Volkhard Kaefer,<sup>†</sup> Johannes-Peter Stasch,<sup>‡</sup> and Roland Seifert<sup>\*†</sup>

<sup>†</sup>Institute of Pharmacology, Hannover Medical School, Hannover, Germany

<sup>‡</sup>Institute of Cardiovascular Research, Bayer HealthCare, Wuppertal, Germany

## S Supporting Information

**ABSTRACT:** Soluble guanylyl cyclase (sGC) regulates several important physiological processes by converting GTP into the second-messenger cGMP. sGC has several structural and functional properties in common with adenylyl cyclases (ACs). Recently, we reported that membranous ACs and sGC are potently inhibited by 2',3'-O-(2,4,6-trinitrophenyl)-substituted purine and pyrimidine nucleoside 5'-triphosphates. Using a highly sensitive high-performance liquid chromatography–tandem mass spectrometry method, we report that highly purified recombinant sGC of rat possesses nucleotidyl cyclase activity. As opposed to GTP, ITP, XTP and ATP, the pyrimidine nucleotides UTP and CTP were found to be sGC substrates in the presence of  $Mn^{2+}$ . When  $Mg^{2+}$  is used, sGC generates cGMP, cAMP, cIMP, and cXMP. In conclusion, soluble “guanylyl” cyclase possesses much broader substrate specificity than previously assumed. Our data have important implications for cyclic nucleotide-mediated signal transduction.



Guanylyl cyclases (GCs) make up a family of enzymes that catalyze the biosynthesis of guanosine 3',5'-cyclic monophosphate (cGMP) from guanosine 5'-triphosphate (GTP). The family consists of two isoforms, the soluble isoform that is expressed in cytoplasm and the particulate or membrane-bound form.<sup>1–3</sup> The soluble GC (sGC) is a heterodimer consisting of an  $\alpha$ -subunit and a  $\beta$ -subunit containing a heme as a prosthetic group.<sup>4</sup> Two sGC isoforms have been identified. The best-studied sGC isoform is termed  $\alpha_1\beta_1$  and is expressed in most tissues.<sup>4</sup> Further subunits have also been cloned, i.e.,  $\alpha_2$ ,  $\alpha_{2i}$  (a splice variant of  $\alpha_2$ ),  $\beta_2$ , and  $\beta_3$ . However, only  $\alpha_2\beta_1$  has been detected in vivo. The  $\alpha_2\beta_1$  isoform is expressed in brain and in fetal tissue.<sup>4</sup> In vitro studies with  $\alpha_2\beta_1$  showed very similar NO and carbon monoxide binding characteristics as well as inhibition by [1,2,4]oxadiazolo[4,3-*a*]quinoxalin-1-one (ODQ) and stimulation by YC-1 {5-[1-(phenylmethyl)-1H-indazol-3-yl]-2-furanmethanol} compared to  $\alpha_1\beta_1$ , although the sequences of  $\alpha_1$  and  $\alpha_2$  are only 27% identical.<sup>5</sup> The discovery of other possible sGC subunit combinations in vivo remains elusive.

Nitric oxide (NO) activates sGC up to 100–400-fold.<sup>4</sup> Stimulation of sGC leads to accumulation of cGMP. cGMP is a second messenger regulating cGMP-dependent protein kinases, phosphodiesterases, and ion channels. cGMP signaling plays an important role in many (patho)physiological processes like smooth muscle relaxation and neurotransmission.<sup>6</sup> Heme of sGC can be oxidized by reactive oxygen species or by ODQ, which is followed by a loss of NO sensitivity.<sup>6–8</sup>

Adenylyl cyclases (ACs) are structurally and functionally related to GCs. Recently, we demonstrated that membranous

ACs (mACs) are very potently inhibited by 2',3'-O-(2,4,6-trinitrophenyl) nucleotides (TNP-nucleotides) and 2'(3')-O-(*N*-methylantraniloyl) nucleotides (MANT-nucleotides).<sup>9–11</sup> For GCs, in 1969, supernatant fractions of rat lung were shown to be inhibited by adenosine 5'-triphosphate (ATP), inosine 5'-triphosphate (ITP), cytidine 5'-triphosphate (CTP), and uridine 5'-triphosphate (UTP),<sup>12</sup> and some years later, sGC purified from rat brain was shown to be inhibited by CTP, UTP, and ATP in a competitive manner.<sup>13</sup> Furthermore, sGC produces adenosine 3',5'-cyclic monophosphate (cAMP)<sup>9,14,15</sup> and bona fide uridine 3',5'-cyclic monophosphate (cUMP)<sup>9</sup> as assessed by a classical radiometric nucleotidyl cyclase (NC) assay. ATP is a mixed-type inhibitor of sGC, indicating that sGC contains an allosteric nucleotide binding site.<sup>15</sup> Moreover, soluble fractions of rat lung generate inosine 3',5'-cyclic monophosphate (cIMP) besides cGMP.<sup>16</sup> Finally, the biosynthesis of cGMP by sGC is also potently inhibited by MANT- and TNP-substituted purine and pyrimidine nucleotides.<sup>9,10</sup>

However, the assumed broader NC activity of sGC was always a matter of controversy because of crude enzyme preparations, impure analytical standards, or cross reactivity of antibodies.<sup>12,16–22</sup> In the present study, for the first time, comprehensive kinetic parameters are obtained for synthesis of seven cyclic purine and pyrimidine nucleotides by highly purified recombinant rat sGC isoform  $\alpha_1\beta_1$ . Because not all NTPs are commercially available as radiolabeled analogues and

Received: August 10, 2011

Revised: November 24, 2011

Published: November 28, 2011



**Table 1. Parameters for the Detection and Identification of cNMPs and MS Standard Tenofovir<sup>a</sup>**

	cAMP	cCMP	cGMP	cIMP	cTMP	cUMP	cXMP	tenofovir
[M + H] <sup>+</sup> ( <i>m/z</i> )	330.1	306.1	346.1	331.1	305.1	307.0	347.1	288.2
quantifier ( <i>m/z</i> )	136.2	112.1	152.1	137.2	127.1	113.1	153.1	176.2
qualifier ( <i>m/z</i> )	119.1	95.0	135.2	110.1	81.0	97.0	136.2	270.2
quantifier/qualifier ratio	1:10	1:6.8	1:3.2	1:5.3	1:3.7	1:1.1	1:3.1	1:1.1
retention time (min)	4.4	2.9	3.3	3.4	3.7	3.1	2.7	3.6

<sup>a</sup>Protonated molecular masses ([M + H]<sup>+</sup>), HPLC retention times, quantifier and qualifier MS/MS fragments, and quantifier:qualifier ratios are given.

structure-based identification of products has not yet been performed, we have developed an analytical method based on high-performance liquid chromatography and tandem mass spectrometry (HPLC–MS/MS) for simultaneous detection and quantitation of seven nucleoside 3',5'-cyclic monophosphates (cNMPs): adenosine 3',5'-cyclic monophosphate (cAMP), cytidine 3',5'-cyclic monophosphate (cCMP), guanosine 3',5'-cyclic monophosphate (cGMP), inosine 3',5'-cyclic monophosphate (cIMP), thymidine 3',5'-cyclic monophosphate (cTMP), uridine 3',5'-cyclic monophosphate (cUMP), and xanthosine 3',5'-cyclic monophosphate (cXMP).

## MATERIALS AND METHODS

NTPs of adenine (2Na·ATP, ≥99%), uracil (3Na·UTP, ≥96%), hypoxanthine (3Na·ITP, 95–97%), and guanine (GTP, ≥95%) as well as triethylamine (TEA), ethylene glycol bis(2-aminoethyl ether)-*N,N,N',N'*-tetraacetic acid (EGTA), Na·cAMP, magnesium chloride, dithiothreitol (DTT), bovine serum albumin (BSA), sodium nitroprusside (SNP), ODQ, dimethyl sulfoxide (DMSO), and sodium acetate were purchased from Sigma-Aldrich (Seelze, Germany). Cytidine 5'-triphosphate (CTP, >99%), xanthosine 5'-triphosphate (XTP, >95%), and thymidine 5'-triphosphate (dTTP, >95%) were obtained from Jena Bioscience (Jena, Germany). Tris(hydroxymethyl)aminomethane hydrochloride (Tris-HCl) was purchased from Merck (Darmstadt, Germany). cGMP, cUMP, cIMP, cCMP, cXMP, and cTMP (cNMP·Na) were supplied by Biolog (Bremen, Germany). Manganese chloride tetrahydrate, hydrochloric acid, and ammonium acetate were purchased from Fluka (Buchs, Germany). Acetonitrile, methanol, and water were supplied by Baker (Deventer, The Netherlands), and acetic acid was purchased from Honeywell/Riedel-de Haën (Seelze, Germany). [ $\alpha$ -<sup>32</sup>P]GTP (3000 Ci/mmol) was obtained from Hartmann Analytic (Braunschweig, Germany). Aluminum oxide N Super 1 was purchased from MP Biomedicals (Eschwege, Germany). Tenofovir was obtained through the National Institute of Health AIDS Research and Reference Program, Division of AIDS (catalog no. 10199) (Bethesda, MD). sGC  $\alpha_1\beta_1$  was purified as described in ref 23.

**Nonradioactive NC Assay of sGC  $\alpha_1\beta_1$ .** Directly before each experiment, the sGC activator SNP was dissolved in a light-protected brown tube in 100 mM sodium acetate (pH 5.0). NC activities were analyzed at 37 °C in a reaction buffer containing 50 mM triethanolamine (TEA) (pH 7.5), 100  $\mu$ M EGTA, 3 mM free Mn<sup>2+</sup> or Mg<sup>2+</sup>, 1 mM DTT, 1 mg/mL BSA, and 100  $\mu$ M SNP or 100  $\mu$ M ODQ [0.3% (v/v) DMSO] and SNP in a final volume of 50  $\mu$ L. The NTP/Me<sup>2+</sup> concentration ranged from 2 to 7500  $\mu$ M. Depending on the analyzed NTP, reaction was initiated by the addition of 0.1–50 ng of purified enzyme. After 5–60 min, assays were stopped when the samples were heated at 95 °C for 10 min. After cooling, mixtures were diluted with 50  $\mu$ L of a 97:3 (v/v) water/

methanol mixture containing 50 mM ammonium acetate, 0.1% (v/v) acetic acid, and 100 ng/mL tenofovir. Denatured protein was precipitated by centrifugation for 10 min at 20000g.

**HPLC–MS/MS Quantitation of NC Assays.** cNMPs were separated using a Series 200 HPLC system (Perkin-Elmer, Norwalk, CT) equipped with a binary pump system, a degasser, and a temperature-controlled autosampler. After the injection of 50  $\mu$ L, analytes were separated by use of a column saver (2.0  $\mu$ m filter, Supelco Analytical, Seelze, Germany), a security guard cartridge (C<sub>18</sub>, 4 mm × 2 mm, Phenomenex, Aschaffenburg, Germany), and a Zorbax Eclipse XDB-C<sub>18</sub> column (50 mm × 4.6 mm, 1.8  $\mu$ m, Agilent Technologies, Böblingen, Germany) at 25 °C. Eluent A consisted of a 3:97 (v/v) methanol/water mixture containing 50 mM ammonium acetate and 0.1% (v/v) acetic acid, and eluent B consisted of a 97:3 (v/v) methanol/water mixture containing 50 mM ammonium acetate and 0.1% (v/v) acetic acid. The flow rate was 0.4 mL/min throughout the chromatographic run. A linear gradient from 100% (v/v) A to 50% (v/v) B was applied between 0 and 5 min followed by re-equilibration of the column at 100% (v/v) A from 5 to 7 min. Tenofovir was used as an internal standard at a final concentration of 50 ng/mL.

Mass detection was performed on an API 3000 triple quadrupole mass spectrometer (ABSciex, Darmstadt, Germany) using selected ion monitoring (SRM) analysis in positive ionization mode. The SRM transitions were detected with a 40 ms dwell time. Parameters of HPLC–MS/MS fragments are listed in Table 1. Ion source settings and collision gas pressure were manually optimized regarding ion source voltage, ion source temperature, nebulizer gas, and curtain gas (ion source voltage of 5500 V, ion source temperature of 350 °C, curtain gas of 15 psi, and collisionally activated dissociation gas of 10 psi). Chromatographic data were collected and analyzed with Analyst version 1.4.1 (ABSciex). Quantitation was performed with nitrogen as the collision gas.

**Radioactive GC Assay.** The sGC activities by means of [ $\alpha$ -<sup>32</sup>P]GTP were assayed as described for a nonradioactive NC assay except that 0.3  $\mu$ Ci of [ $\alpha$ -<sup>32</sup>P]GTP was added per assay. Samples were supplemented with 50  $\mu$ L of 2.2 M hydrochloric acid and centrifuged for 10 min at 20000g to sediment denatured protein. To separate [<sup>32</sup>P]cGMP from the remaining [ $\alpha$ -<sup>32</sup>P]GTP, we loaded samples onto columns containing 1.4 g of neutral aluminum oxide and eluted [<sup>32</sup>P]cGMP using 100 mM Tris-HCl buffer (pH 7.5).<sup>23</sup> Čerenkov radiation was measured with a Tri-Carb 2810 TR liquid scintillation analyzer (Perkin-Elmer) for 1 min.

**Statistics.** Data are presented as means ± the standard error of the mean (SEM) and are based on at least six independent experiments. GraphPad Prism version 5.01 (GraphPad, San Diego, CA) was used for nonlinear regression and calculation of mean, SEM, K<sub>v</sub>, K<sub>M</sub>, V<sub>max</sub>, and IC<sub>50</sub> values.

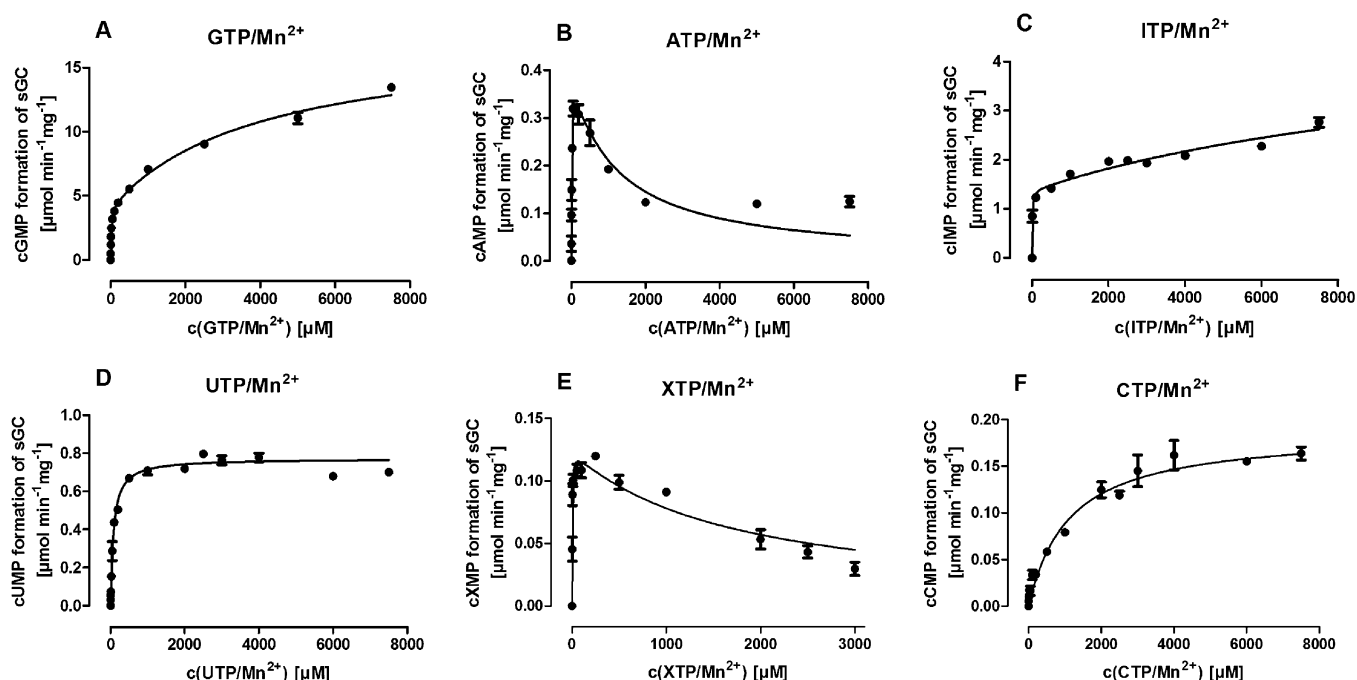


**Figure 1.** Kinetics of formation of cNMP by sGC in the presence of  $\text{Mn}^{2+}$ . sGC (0.1–20 ng of sGC per tube) was incubated with 100  $\mu\text{M}$  SNP and various concentrations of NTP/ $\text{Mn}^{2+}$  at 37 °C. After 5–20 min, depending on the investigated NTP, reactions were stopped by heat and analyzed via HPLC–MS/MS. Data were plotted by use of nonlinear regression. For GTP (A) and ITP (C), a model based on two substrate binding sites was used. For ATP (B) and XTP (E), data were best described using a substrate inhibition model. Results for UTP (D) and CTP (F) were best described by monophasic modeling. Please note in all panels the different scales of the y-axes and in (E) the different x- and y-axes. Data shown are the means  $\pm$  SEM of six independent experiments. The results of the nonlinear regression analysis of data are listed in Table 2.

**Table 2. Michaelis–Menten Kinetic Parameters of sGC for Various NTPs Using  $\text{Mn}^{2+}$  as a Cofactor<sup>a</sup>**

	ATP	CTP	GTP	ITP	TTP	UTP	XTP
$K_{M1}$ ( $\mu\text{M}$ )	$14.8 \pm 0.2$	$1144 \pm 148$	$14.2 \pm 1.6$	$6.6 \pm 1.9$	nd	$80.8 \pm 6.2$	$2.5 \pm 0.5$
$V_{\max1}$ ( $\mu\text{mol min}^{-1} \text{mg}^{-1}$ )	$0.40 \pm 0.02$	$0.19 \pm 0.01$	$4.1 \pm 0.15$	$1.4 \pm 0.1$	nd	$0.77 \pm 0.01$	$0.1 \pm 0.01$
$K_{M2}$ ( $\mu\text{M}$ )	–	–	$4819 \pm 552$	13189	nd	–	–
$V_{\max2}$ ( $\mu\text{mol min}^{-1} \text{mg}^{-1}$ )	–	–	$13.5 \pm 0.7$	$3.4 \pm 1.5$	nd	–	–
$V_{\max1}$ of GC (%)	9.8	4.6	100	34.1	–	18.8	2.4
$K_i$ ( $\mu\text{M}$ )	$1167 \pm 213$						$1696 \pm 276$

<sup>a</sup>NC activities were analyzed as described in Materials and Methods. sGC (1–20 ng per tube) was incubated with 2–7500  $\mu\text{M}$  NTP/ $\text{Mn}^{2+}$  (2–3000  $\mu\text{M}$  XTP) in the presence of 100  $\mu\text{M}$  SNP and 3 mM  $\text{Mn}^{2+}$  ions at 37 °C for 5–20 min depending on the analyzed NTP. Apparent  $K_M$ ,  $K_i$ , and  $V_{\max}$  values represent the means  $\pm$  SEM of at least six independent experiments shown in Figure 1 and are given in alphabetical order of NTPs. Curves were analyzed by nonlinear regression using Prism version 5.0. nd, not detected.

## RESULTS

**Comparison of the Radioactive Cyclase Assay versus the HPLC–MS/MS-Based Cyclase Assay.** NC assays are routinely performed using methods based on radiolabeled substrates or antibodies.<sup>9,15,24,25</sup> We developed an HPLC–MS/MS method for the simultaneous quantitation of seven cNMPs. To compare the radioactive and nonradioactive quantitation method, we incubated 1 ng of sGC per tube for 20 min at 37 °C with various concentrations of GTP/ $\text{Mn}^{2+}$ . Figure S1 of the Supporting Information illustrates that both methods achieved nearly identical Michaelis–Menten plots. The GC activity of sGC showed a saturation plot with a  $K_M$  of  $28.8 \pm 3.7$   $\mu\text{M}$  and a  $V_{\max}$  of  $3.7 \pm 0.1$   $\mu\text{mol min}^{-1} \text{mg}^{-1}$  for the radioactive assay and a  $K_M$  of  $47.1 \pm 4.7$   $\mu\text{M}$  and a  $V_{\max}$  of  $3.6 \pm 0.1$   $\mu\text{mol min}^{-1} \text{mg}^{-1}$  for the HPLC–MS/MS method. Having validated the HPLC–MS/MS method, we performed all further experiments via this approach.

**Time Courses of sGC Activity.** Incubation of 0.1 ng of sGC per tube and 200  $\mu\text{M}$  GTP/ $\text{Mn}^{2+}$  in the presence of 3 mM

free  $\text{Mn}^{2+}$  ions and 100  $\mu\text{M}$  SNP at 37 °C resulted in linear cGMP production for 90 min (Figures S2A and S3A of the Supporting Information). As expected, sGC showed a large increase in the level of GTP cyclization. The activity of sGC was 20-fold higher in the presence of  $\text{Mn}^{2+}$  than in the presence of  $\text{Mg}^{2+}$ . However, other substrates were also accepted, although activities were significantly lower. In the presence of  $\text{Mg}^{2+}$ , sGC converted GTP, ATP, ITP, and XTP. In the presence of  $\text{Mn}^{2+}$ , sGC additionally cyclized UTP and CTP. In comparison to GTP, other NTPs showed a distinct time-dependent saturation. Specifically for NTPs other than GTP, the linearity of reaction was lost after 5–20 min, depending on the NTP studied. For both experimental conditions, a thymidyl cyclase (TC) activity was not observed. All further experiments were performed under linear conditions to yield accurate Michaelis–Menten plots.

**Enzyme Kinetics of sGC.** We analyzed the Michaelis–Menten kinetics of sGC for GTP, ATP, ITP, UTP, CTP, and XTP in a concentration range of 2–1000  $\mu\text{M}$  in the presence of

**Table 3. Michaelis–Menten Kinetic Parameters of sGC for Various NTPs Using  $Mg^{2+}$  as a Cofactor<sup>a</sup>**

	ATP	CTP	GTP	ITP	TTP	UTP	XTP
$K_M$ ( $\mu M$ )	5548 $\pm$ 1.12	nd	119.1 $\pm$ 13.7	796 $\pm$ 90	nd	nd	241 $\pm$ 27
$V_{max}$ ( $\mu mol\ min^{-1}\ mg^{-1}$ )	0.9 $\pm$ 0.1	nd	2.2 $\pm$ 0.5	4.9 $\pm$ 0.1	nd	nd	0.008 $\pm$ 0.0003
$V_{max}$ of GC (%)	40.9	–	100	222	–	–	0.4

<sup>a</sup>NC activities were analyzed as described in Materials and Methods. sGC (1–50 ng per tube) was incubated with 2–7500  $\mu M$  NTP/ $Mg^{2+}$  (2–3000  $\mu M$  XTP) in the presence of 100  $\mu M$  SNP and 3 mM  $Mg^{2+}$  ions at 37 °C for 5–10 min depending on the analyzed NTP. Apparent  $K_M$ ,  $K_i$ , and  $V_{max}$  values represent the means  $\pm$  SEM of at least six independent experiments shown in Figure 2 and are given in alphabetical order of NTPs. Curves were analyzed by nonlinear regression using Prism version 5.0. nd, not detected.

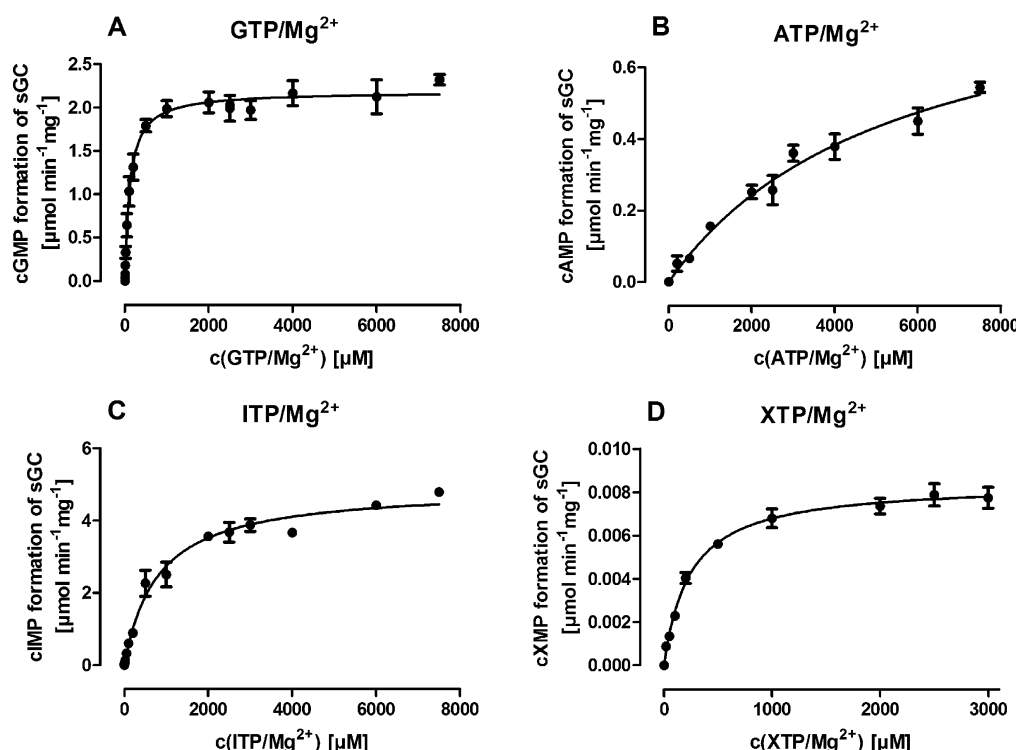


**Figure 2.** Kinetics of formation of cNMP by sGC in the presence of  $Mg^{2+}$ . sGC (1–50 ng per tube) was incubated with 100  $\mu M$  SNP and various concentrations of NTP/ $Mg^{2+}$  at 37 °C. After 5–20 min, depending on the investigated NTP, reactions were stopped with heat and analyzed via HPLC–MS/MS. Data were plotted by use of nonlinear regression. For all panels, data were best described using a monophasic model. A pyrimidinyl cyclase activity was not detected. Please note in all panels the different scales of the y-axes and in panel D the different x- and y-axes. Data shown are the means  $\pm$  SEM of six independent experiments. The results of the nonlinear regression analysis of data are listed in Table 3.

3 mM free  $Mn^{2+}$  and 100  $\mu M$  SNP. With regard to  $V_{max}$ , we observed a descending order of cNMP formation: cGMP > cIMP > cUMP > cAMP > cCMP  $\approx$  cXMP (Figure 1). With regard to  $K_M$ , we found an ascending order: XTP < ITP < GTP  $\approx$  ATP  $\ll$  UTP  $\ll$  CTP. ATP and XTP exhibited substrate inhibition, and XTP and ITP showed a considerably lower  $K_M$  than GTP. A summary of the kinetic properties of sGC is shown in Table 2. In the presence of  $Mn^{2+}$  and in the case of GTP and ITP, we additionally observed that catalytic activity in the high micromolar concentration range (500–1000  $\mu M$ ) was not appropriately described by using a single-site binding model. Therefore, we additionally investigated saturation behavior of all NTPs in the millimolar concentration range (1000–7500  $\mu M$ ; for XTP, 1000–3000  $\mu M$ ). For GTP and ITP, data points were better described by use of a model with a biphasic saturation curve (Figure 1 and Table 2). For pyrimidine NTPs, curve fitting using a monophasic regression curve was sufficient even at millimolar concentrations.

When  $Mn^{2+}$  was replaced with  $Mg^{2+}$ , the NC activity of sGC was reduced except for that of ITP, and  $K_M$  was increased for all NTPs. With regard to  $V_{max}$ , we observed a descending order of

cNMP formation: cIMP > cGMP  $\gg$  cAMP  $\gg$  cXMP (Table 3). For  $K_M$  values, we found an ascending order: GTP < XTP < ITP  $\ll$  ATP. In the case of GTP, GC activity decreased to half of the activity with  $Mn^{2+}$ , and  $K_M$  increased 8-fold. Surprisingly, for ITP in the presence of  $Mg^{2+}$ ,  $V_{max}$  was even 2-fold higher than for GTP. For all NTPs, best fits were achieved by Michaelis–Menten plots including only one binding site. A pyrimidinyl cyclase activity in the presence of  $Mg^{2+}$  was not observed.

**Inhibition of sGC's GC Activity by ATP.** The substrate inhibition curves for ATP indicated an inhibitory effect on cAMP synthesis (Figure 1B). ATP is a mixed-type inhibitor for NO-stimulated sGC activity.<sup>15</sup> We analyzed the influence of ATP on 1 mM GTP cyclization by sGC (0.1–1 ng per tube) at 37 °C for 20 min in the presence of  $Mn^{2+}$  or  $Mg^{2+}$ . As illustrated in Figure S4A of the Supporting Information, ATP reduced GC activity with an  $IC_{50}$  of 204.7  $\pm$  1.2  $\mu M$  in the presence of  $Mn^{2+}$  and an  $IC_{50}$  of 252.4  $\pm$  1.0  $\mu M$  in the presence of  $Mg^{2+}$ . Moreover, even in the presence of 1 mM GTP, an AC activity was observed (Figure S4B of the Supporting Information). Kinetic studies revealed a substrate



**Table 4. Substrate Specificity of sGC for Various NTP/Me<sup>2+</sup> Forms under Basal, NO-Activated, and Heme-Oxidized Conditions<sup>a</sup>**

		ATP	CTP	GTP	ITP	TTP	UTP	XTP
Mn <sup>2+</sup>	basal	1.7 ± 0.2	1.1 ± 0.1	661.7 ± 58.9	36.6 ± 1.5	nd	2.5 ± 0.8	0.7 ± 0.08
	SNP	240.8 ± 20.0	8.9 ± 2.1	3272 ± 464	1232 ± 35	nd	92.4 ± 8.6	16.2 ± 6.5
	ODQ and SNP	1.6 ± 0.1	0.3 ± 0.04	965 ± 120	39.3 ± 1.4	nd	2.4 ± 0.2	0.6 ± 0.1
Mg <sup>2+</sup>	basal	nd	nd	28 ± 0.01	5.2 ± 0.01	nd	nd	nd
	SNP	4.4 ± 0.4	nd	2850 ± 108	1323 ± 38	nd	nd	0.4 ± 0.1
	ODQ and SNP	nd	nd	20 ± 0.6	5.6 ± 0.6	nd	nd	nd

<sup>a</sup>NC activities were analyzed as described in Materials and Methods. sGC (50 ng per tube) was incubated with 200 μM NTP/Me<sup>2+</sup> in the presence of 100 μM SNP or 100 μM ODQ with SNP and 3 mM Me<sup>2+</sup> ions at 37 °C for 60 min. Values represent the means ± SD of at least two independent experiments performed in duplicate and are given in alphabetical order of NTPs and in units of nanomoles per minute per milligram. nd, not detected. Please note that experiments were not performed under linear conditions.

inhibition with the following parameters for Mn<sup>2+</sup>:  $K_M = 306 \pm 88.8 \mu\text{M}$ ,  $V_{\text{max}} = 0.23 \pm 0.04 \mu\text{mol min}^{-1} \text{mg}^{-1}$ , and  $K_i = 1094 \pm 329 \mu\text{M}$ . For Mg<sup>2+</sup>, the determination of kinetic parameters was ambiguous. Finally, our data are in accord with those published for inhibition of sGC via ATP.<sup>15</sup>

**Substrate Specificity of Basal and Ferric sGC.** To investigate whether sGC's nucleotidyl cyclase activity can also be observed under basal conditions and with ferric sGC, we incubated 50 ng of sGC per tube and 200 μM NTP/Me<sup>2+</sup> in the presence of 3 mM free Me<sup>2+</sup> ions at 37 °C for 60 min. As documented in Table 4, sGC exhibited basal nucleotidyl cyclase activity for GTP, ATP, ITP, CTP, UTP, and XTP with Mn<sup>2+</sup> as the divalent cation. No TC activity was detected. The highest basal activity in the presence of Mn<sup>2+</sup> was found for GTP, followed by ITP, UTP, ATP, and XTP. In the presence of Mg<sup>2+</sup>, basal activities were substantially lower and NC activities could be detected for only GTP and ITP. SNP exhibited differential effects on basal activities. In the presence of Mn<sup>2+</sup>, SNP increased GC activity 5-fold. The strongest stimulation was found for AC activity (142-fold) followed by UC activity (37-fold), IC activity (33-fold), XC activity (23-fold), and CC activity (8-fold). In the presence of Mg<sup>2+</sup>, stimulation of GC activity by SNP was 100-fold and that for IC activity 254-fold. For CTP and UTP in the presence of Mg<sup>2+</sup>, no pyrimidinyl cyclase activity was observed. However, with ATP and XTP, some SNP-stimulated activity was observed in the presence of Mg<sup>2+</sup>. Treatment of sGC with 100 μM ODQ oxidizes Fe<sup>II</sup> of the heme moiety to Fe<sup>III</sup>, resulting in NO insensitivity.<sup>8</sup> ODQ reduced SNP-stimulated NC activities and did so differentially. In the presence of Mn<sup>2+</sup>, ODQ reduced CC activity to one-third of basal activity, whereas in the case of GTP and ITP, a small stimulatory effect of SNP was still observed. With ATP, UTP, and XTP, NC activity was reduced slightly below basal values. In the presence of Mg<sup>2+</sup>, ODQ abrogated SNP-stimulated AC and XC activity. Under these conditions, GC activity was reduced below the basal level, and in the case of IC activity, a small stimulatory effect of SNP was still evident.

## DISCUSSION

**Comparison of the Radioactive Cyclase Assay versus the HPLC–MS/MS-Based Cyclase Assay.** The NC activity of GC has always been highly controversial on the basis of impure enzyme preparations, analytical standards, or the cross reactivity of the used antibodies.<sup>12,16–21</sup> Even today, quantitation of cAMP and cGMP followed by an enzyme immunoassay can be problematic, particularly with regard to cross reactivity.<sup>22</sup> A further problem with radiometric assays is the isotope dilution with higher NTP concentrations followed

by a loss of sensitivity.<sup>15</sup> This loss of sensitivity can be partially compensated by drastically increasing the amount of radioactively labeled NTP, but such a methodological procedure does not find broad acceptance among scientists. Therefore, we established a quantitation method based on HPLC–MS/MS with high sensitivity and selectivity. In contrast to the methods mentioned above, for this technique, all NTPs are commercially available and do not have to be radiolabeled. Our method also allows for unequivocal molecular identification of any given cNMP by specific ratios of molecule quantifiers and identifiers. Importantly, higher substrate concentration ranges can easily be analyzed because an isotope dilution is missing. As illustrated in Figure S1 of the Supporting Information, our HPLC–MS/MS method achieved results very similar to those of the classical, radioactive assay.

**Time Courses of sGC Activity.** Taking advantage of the HPLC–MS/MS system, we investigated the substrate specificity of sGC. To receive exact results, we used only enzyme preparations of the highest available purity.<sup>23</sup> By investigating the time-dependent generation of cNMPs, we could confirm that GTP cyclization is linear over time for at least 90 min<sup>19</sup> and cGMP synthesis is the most effective reaction compared to other cyclization reactions. However, sGC accepted further substrates. The formation rate in descending order was as follows: cGMP ≫ cIMP > cAMP > cUMP > cXMP > cCMP. In contrast to cGMP, other cNMPs showed a distinct time-dependent saturation of cNMP formation. This saturation was not due to a lack of substrate as nucleotide concentrations were well above the  $K_M$ . Apparently, GTP is the most effective NTP in terms of stabilization of a catalytically active sGC: GTP > ITP > ATP > UTP > CTP > XTP. In the case of Mg<sup>2+</sup>, sGC's substrate specificity was reduced to purine NTPs (GTP, ATP, ITP, and XTP). The stabilization effectiveness of NTPs in the presence of Mg<sup>2+</sup> in descending order is as follows: GTP ≫ ITP > ATP ≈ XTP. In general, with purine NTPs, we observed a higher cyclase activity than with pyrimidine NTPs in terms of  $V_{\text{max}}$ , which is probably due to the strong structural similarity to GTP. Under all experimental conditions, a TC activity was not observed. In comparison to other NTPs, dTTP lacks the 2'-hydroxyl group at the ribosyl moiety. However, Garbers et al.<sup>16</sup> showed that the supernatant fraction of rat lung preparations formed 2'-deoxyguanosine 3',5'-cyclic monophosphate from dGTP with 50% effectiveness compared to GC activity. The combination of a missing 2'-hydroxyl group and a missing purine base is probably responsible for a lack of activity of sGC on dTTP.

**Enzyme Kinetics of sGC.** So far, no X-ray crystal structure of full-length sGC has been determined. Current sGC models

**Table 5. Comparison of Reported Michaelis–Menten Kinetic Parameters of sGC for NTPs**

substrate	$K_M$ ( $\mu\text{M}$ )	$V_{\max}$ ( $\mu\text{mol min}^{-1} \text{mg}^{-1}$ )	activator	source	method	ref
GTP/ $\text{Mn}^{2+}$	15	0.29	SNP	bovine lung	radiometric	9
GTP/ $\text{Mn}^{2+}$	—	0.9–1.8	SNP	bovine lung	radiometric	35
GTP/ $\text{Mn}^{2+}$	10	0.1	NO gas	bovine lung	radiometric	37
GTP/ $\text{Mg}^{2+}$	44	11.8	DEA/NO	rat <sub>rec.</sub> in Sf9 cells	immunoassay	15
GTP/ $\text{Mg}^{2+}$	156	0.75	SNP	bovine lung	immunoassay	25
GTP/ $\text{Mg}^{2+}$	21	1.396	SNAP	rat <sub>rec.</sub> in Sf21 cells	radiometric	29
GTP/ $\text{Mg}^{2+}$	—	1.2–2.4	SNP	bovine lung	radiometric	35
GTP/ $\text{Mg}^{2+}$	85–120	0.4	NO gas	bovine lung	radiometric	37
GTP/ $\text{Mg}^{2+}$	49.8	11.642	NOC-12	human <sub>rec.</sub> in Sf9 cells	HPLC–UV	30
GTP/ $\text{Mg}^{2+}$	119	1.49	DEA/NO	rat <sub>rec.</sub> in Sf9 cells	radiometric	31
GTP/ $\text{Mg}^{2+}$	43	1.330	NOC-12	bovine lung	HPLC–UV	32
GTP/ $\text{Mg}^{2+}$	22	11.5	NO gas	bovine lung	radiometric	33
GTP/ $\text{Mg}^{2+}$	—	28.2	NO gas	bovine lung	immunoassay	34
ATP/ $\text{Mn}^{2+}$	15	0.015	SNP	bovine lung	radiometric	9
ATP/ $\text{Mg}^{2+}$	52	0.63	DEA/NO	rat <sub>rec.</sub> in Sf9 cells	immunoassay	15
ITP/ $\text{Mn}^{2+}$	—	10% of GC <sup>a</sup>	—	rat lung	radiometric	16
UTP/ $\text{Mn}^{2+}$	25	0.0092	SNP	bovine lung	radiometric	9

<sup>a</sup>Substrate concentration of 0.1 mM. Abbreviations: DEA/NO, diethylamine nonoate; NOC-12, N-ethyl-2-(1-ethyl-2-hydroxy-2-nitrosohydrazino)-ethanamine; SNAP, S-nitroso-N-acetyl-DL-penicillamine; rec., recombinant.

are based on crystal structures of the catalytic domain.<sup>26,27</sup> The catalytic site is localized in the C-terminus of the  $\alpha$ - and  $\beta$ -subunits. Both domains are required for catalytic activity. sGC from *Chlamydomonas reinhardtii* contains two active sites that act cooperatively, providing evidence that the active sites interact with each other.<sup>27</sup> However, in the second binding site, basic residues, which are responsible for coordinating  $\beta$ - and  $\gamma$ -phosphate binding of NTPs and for maintaining the transition state, and two aspartate residues, which are required for metal coordination, are missing. Thus, this binding site is predicted to lack catalytic activity.<sup>27,28</sup> Therefore, sGC is suggested to exhibit a nucleotide-like (pseudosymmetric) binding site and a putative catalytic site.<sup>15</sup>

By using highly purified sGC and HPLC–MS/MS quantitation, we could show that in vitro, sGC has broader substrate specificity than previously assumed. As expected, we confirm that the dominant cyclase activity of sGC was the GC activity. We found kinetic parameters ( $K_M = 14.2 \mu\text{M}$ , and  $V_{\max} = 4.1 \mu\text{mol min}^{-1} \text{mg}^{-1}$ ) in the presence of  $\text{Mn}^{2+}$  comparable to literature kinetic parameters with a  $K_M$  within the range of 10–156  $\mu\text{M}$  and a  $V_{\max}$  with the range of 0.75–28.2  $\mu\text{mol min}^{-1} \text{mg}^{-1}$  (Table 4). We also could confirm that using  $\text{Mg}^{2+}$  ions, the specific activity of rat sGC is ~50% lower than that of bovine sGC.<sup>23</sup>

In the presence of  $\text{Mn}^{2+}$ , ATP, CTP, ITP, UTP, and XTP were substrates of sGC, too. In comparison to that of GTP,  $V_{\max}$  values of the other NTPs were significantly lower. An AC activity of bovine lung sGC has been described by Gille et al. with a  $K_M$  of 15  $\mu\text{M}$  and a  $V_{\max}$  of 15  $\text{nmol min}^{-1} \text{mg}^{-1}$ .<sup>9</sup> We found a comparable  $K_M$  of 14.8  $\mu\text{M}$  but a significantly higher  $V_{\max}$  of 400  $\text{nmol min}^{-1} \text{mg}^{-1}$ . This difference may be explained by different incubation temperatures (30 °C vs 37 °C), different enzyme sources, or longer periods of storage of bovine sGC. Gille et al. also reported a significantly lower  $V_{\max}$  for GC activity (Table 5), which he suggested was due to the specific commercial enzyme preparation used.<sup>9</sup> Gerzer et al. showed that at 37 °C the specific AC activity of bovine sGC was 630  $\text{nmol min}^{-1} \text{mg}^{-1}$  in the presence of  $\text{Mn}^{2+}$ .<sup>19</sup> Moreover, we could confirm that ATP exhibits substrate inhibition at millimolar concentrations.<sup>15</sup>

Gille et al. also described a bona fide UC activity with a  $K_M$  of 25  $\mu\text{M}$  and a  $V_{\max}$  of 9.2  $\text{nmol min}^{-1} \text{mg}^{-1}$  in a radiometric assay.<sup>9</sup> We determined a  $K_M$  of 80.8  $\mu\text{M}$  and a significantly higher  $V_{\max}$  of 770  $\text{nmol min}^{-1} \text{mg}^{-1}$  using the structure-based HPLC–MS/MS assay. Besides GC, AC, and UC activity, we found that sGC also catalyzed the formation of cIMP with a  $K_M$  of 6.6  $\mu\text{M}$  and a  $V_{\max}$  of 1.4  $\mu\text{mol min}^{-1} \text{mg}^{-1}$ . An IC activity of sGC was formerly described by Garbers et al. amounting to 10% of the GC activity using 0.1 mM ITP, but kinetic parameters were not determined.<sup>16</sup> These parameters are first described here. The differences can be explained by the facts that Garbers et al. did not stimulate sGC by any NO donor and reactions were conducted at 30 °C. The high IC activity documented in this paper explains that Chang et al. reported a considerable inhibition of GC activity by ITP.<sup>29</sup> Interestingly, the  $V_{\max}$  of IC activity was not largely affected when  $\text{Mn}^{2+}$  was replaced with  $\text{Mg}^{2+}$  and cyclase activity was even higher than for GTP. We also found for the first time that in the presence of  $\text{Mg}^{2+}$  and  $\text{Mn}^{2+}$  sGC accepted XTP as a substrate and in the presence of  $\text{Mn}^{2+}$  sGC accepted CTP. Although the CC and XC activity of sGC has not yet been reported, probably because it is low, Zwiller et al.<sup>13</sup> demonstrated that CTP and UTP inhibited GC activity in a competitive manner. This can be explained by the fact that CTP and UTP bind to the catalytic site and are substrates of sGC.

We found that for GTP and ITP saturation data in the presence of  $\text{Mn}^{2+}$  ions were best fitted using a model with two binding sites. When  $\text{Mn}^{2+}$  ions were replaced with  $\text{Mg}^{2+}$  ions, catalysis became monophasic. Indeed, it is known that one sGC molecule binds two molecules of GTP in the presence of  $\text{Mn}^{2+}$  using equilibrium dialysis.<sup>38</sup> Yazawa and co-workers<sup>38</sup> suggested a high-affinity site serving as catalytic site and a low-affinity site for regulation. Derbyshire et al.<sup>15</sup> showed that the NO-independent activator of sGC YC-1 and ATP bind to distinct sites and that the allosteric nucleotide binding site is located at the C-terminus of sGC. We could confirm that sGC possesses two nucleotide binding sites. We suggest that the catalytic site accepts ITP, ATP, XTP, UTP, and CTP apart from GTP. A second allosteric binding site regulates sGC activity. Binding of ATP and XTP in the millimolar concentration range to the

allosteric site results in an inhibition of the catalytic domain. Binding of GTP and ITP to the allosteric site leads to a stabilization of the active conformation, so that sGC exhibits higher GC and IC activity. Figure 3 illustrates formation of cNMP by sGC according to the two-site model.

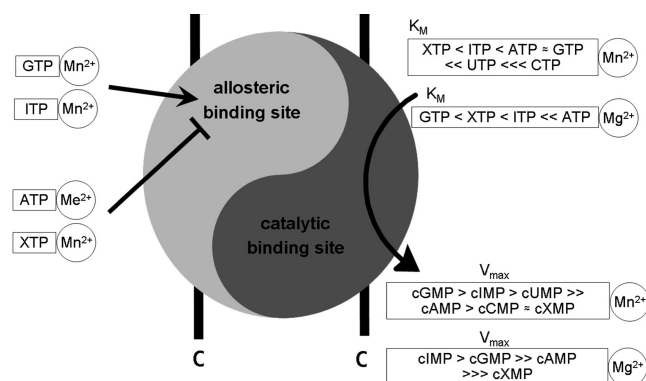


**Figure 3.** Model of the sGC substrate affinity and catalytic activity. Illustrated is the C-terminus of sGC that contains two nucleotide binding sites. Depending on the divalent cation, sGC exhibits distinct  $K_M$  values for NTPs at the catalytic domain in ascending order as indicated. Additionally, sGC has an allosteric (pseudosymmetric) binding site that is regulated by ATP/Me<sup>2+</sup>, XTP/Mn<sup>2+</sup>, ITP/Mn<sup>2+</sup>, and GTP/Mn<sup>2+</sup> in the millimolar concentration range. ATP/Me<sup>2+</sup> and XTP/Mn<sup>2+</sup> inhibit the catalytic domain, while GTP/Mn<sup>2+</sup> and ITP/Mn<sup>2+</sup> stabilize the GC and IC activity of sGC, respectively.

**Substrate Specificity of Basal and Ferric sGC.** NC activity could also be unequivocally detected under basal conditions and with ferric sGC (Table 4), although large amounts of enzyme were required. Under basal and activated conditions, we observed the same order of cNMP formation as shown in Figures S2 and S3 of the Supporting Information. However, depending on the analyzed NTP, sGC exhibited distinct profiles of activation by SNP. The substrate-dependent stimulation of sGC by NO is a first hint of the notion that in intact cells, sGC discriminates among various substrates and that the resulting cNMPs possess different functions. This concept is further corroborated by the finding that the oxidant ODQ differentially affected NC activities. The differential effects of ODQ depended also on the specific cation used. Apparently, heme oxidation in sGC results in a propagated conformational change to the catalytic site that differentially interferes with the binding and turnover of specific NTPs. Thus, ATP, ITP, XTP, CTP, and UTP are not just simple substitutes for GTP at sGC but substrates with specific functional properties in their own right. Future studies will have to elaborate the precise kinetic parameters of basal and ODQ-inhibited NC activities of sGC with various NTPs. We anticipate that this analysis will unmask very intriguing differences between the various NTPs. However, these studies will be quite challenging because high sGC concentrations will be needed for several substrates, and linear conditions will have to be ensured. The sensitivity of the mass spectrometer used in this study (API 3000, ABSciex) will probably not be sufficient for all analyses, and we may have to switch to the more sensitive 5500 QTrap instrument (ABSciex). According to our experience with cNMP quantitation, the 5500 QTrap instrument is 5–10-fold more sensitive than the API 3000 instrument.

**Context of the CC Activity of sGC with Previously Reported CC Activities.** The existence of a mammalian CC activity was suggested 35 years ago,<sup>39</sup> but there were substantial problems with the separation of educt and product on the alumina columns.<sup>40</sup> These problems, together with problems related to the questionable specificity of cCMP-detecting antibodies (reviewed in ref 41), have resulted in very little research of CC. The biochemical properties of previously reported tentative CC activities<sup>42–44</sup> do not fit with the properties of sGC reported here. It should be noted that the previously performed studies of CC activity were performed with crude enzyme preparations. Thus, there could have been multiple forms of interference with the detection methods used, and the molecular identity of the CC had remained elusive in the previous studies. To the best of our knowledge, this is the first report describing a CC activity of a highly purified, well-validated, and clearly defined mammalian enzyme tested previously in other studies.<sup>23,45</sup>

Using highly purified bacterial “adenylyl” cyclase toxins as model NCs, we have recently developed a sensitive and specific radiometric method for the detection of cCMP, cUMP, and cIMP formation.<sup>24</sup> When very high concentrations of toxins are used, cCMP, cUMP, and cIMP formation can even be detected by HPLC.<sup>24</sup> As a further advancement, here, we developed a sensitive and specific combined HPLC–MS/MS method for the detection of cCMP, cUMP, and cIMP formation. With this methodology, we unequivocally showed that highly purified soluble “guanylyl” cyclase exhibits broader substrate specificity than previously assumed. Most strikingly, sGC synthesizes cCMP and cUMP in the presence of Mn<sup>2+</sup>. Notably, too, sGC generates relatively large amounts of cIMP in the presence of Mn<sup>2+</sup> and Mg<sup>2+</sup>. Thus, our data raise the question of whether the rather broad purinyl and pyrimidinyl cyclase activity of sGC is relevant in intact cells.

**Possible Roles of cCMP, cUMP, and cIMP as Second Messengers.** A previous study suggested the physiological existence of cCMP, cUMP, and cIMP in tissues using fast atom bombardment mass spectrometry,<sup>46,47</sup> but the precision and specificity of this method may have been insufficient for unequivocal detection of these cyclic nucleotides. So far, the results of the Newton group have not yet been confirmed independently by another group. In addition, cNMP quantitation is not possible with fast atom bombardment. It will be important to assess cellular cCMP and cUMP concentrations in direct comparison with cAMP and cGMP concentrations. Immunological methods are problematic.<sup>41</sup> However, the HPLC–MS/MS method described here is suitable for quantitation and identification of cNMPs, using specific qualifiers and quantifiers for any given cNMP (Table 1). In forthcoming studies, we will apply our HPLC–MS/MS method to the detection of cCMP, cUMP, and cIMP in intact cells. Because of the clear discrimination among all cNMPs in terms of HPLC retention time and MS/MS fragmentation patterns, we now have the option to simultaneously detect and quantitate seven cNMPs (cAMP, cCMP, cGMP, cIMP, cTMP, cUMP, and cXMP).

cCMP was thought to be involved in the regulation of cell growth, proliferation, tissue development, and modulation of immune responses, but several issues such as questionable membrane penetration of cCMP and very low cCMP concentrations (as low as 100 nM) used to elicit biological effects hampered the interpretation of data and resulted in overall skepticism in the scientific community (reviewed in ref



41). Later, a membrane-permeable cCMP analogue at rather high concentrations (300  $\mu$ M to 1 mM) was shown to regulate the production of superoxide anion in human neutrophils in a stimulus-dependent manner, but the underlying mechanisms remained elusive.<sup>48</sup> Additionally, the purity of the previously used cCMP analogue was of concern. More recently, Desch et al.<sup>49</sup> have shown that a highly purified membrane-permeable cCMP analogue induces vascular smooth muscle relaxation via cGMP-dependent protein kinase and the IRAG protein. Evidence of this mechanism was convincingly provided by the use of corresponding gene knockout animals. Additionally, cCMP and cUMP show different manners of degradation by various purified mammalian phosphodiesterases.<sup>50</sup> Most strikingly and in marked contrast to cUMP, cCMP is resistant to degradation by all phosphodiesterases examined so far. This finding could imply that even with low rates of generation of cCMP by a cCMP-forming enzyme (such as sGC), substantial cellular cCMP concentrations could build up, allowing for substantial biological effects to occur. Moreover, cCMP and cUMP differentially activate cGMP-dependent protein kinase and two isoforms of cAMP-dependent protein kinase.<sup>51</sup> Intriguingly, several publications described an activation of cAMP signaling pathways following NO activation of sGC in intact cells<sup>52–54</sup> and elimination of cGMP shows complex interaction with cAMP.<sup>55</sup> A responsible enzyme has not yet been found, but with respect to our data, sGC's AC activity is a likely candidate. In support of the possible physiological relevance of pyrimidyl cyclase activity of sGC, the bacterial adenyl cyclase toxins CyaA from *Bordetella pertussis* and edema factor from *Bacillus anthracis* also possess CC and UC activity.<sup>24</sup> Moreover, dissociations between edema factor-induced cAMP accumulation and biological effects have been observed in several systems, lending support to the concept that second messengers other than cAMP contribute to the toxin effects.<sup>56</sup>

**Role of  $Mn^{2+}$  in sGC Regulation.** At first glance,  $Mn^{2+}$  is unlikely the substrate cation cofactor of sGC because the concentration of intracellular  $Mg^{2+}$  in vivo is some 2–3 orders of magnitude higher than that of  $Mn^{2+}$ .<sup>36</sup> However,  $Mn^{2+}$  also plays a critical role for important enzymes such as pyruvate carboxylase<sup>57</sup> and mitochondrial superoxide dismutase.<sup>58</sup> While  $Mn^{2+}$  toxicity in humans is well-documented, very little is known about the symptoms of  $Mn^{2+}$  deficiency, which is also due to methodological problems.<sup>59</sup> However, studies with hemodialysis patients suggest that  $Mn^{2+}$  deficiency is associated with increased mortality.<sup>60</sup> Additionally, a sufficient  $Mn^{2+}$  supply is important for proper fetal development.<sup>61</sup>

$Mn^{2+}$  may be present at higher concentrations in vivo in distinct compartments or microdomains in which sGC resides. The  $\alpha_2$  subunit of sGC has already been shown to be enriched in the postsynaptic site of neurons.<sup>62</sup> For soluble AC, it is known that cAMP signaling is regulated in discrete intracellular compartments such as focal cytoplasm points, mitochondria, and the nucleus.<sup>63</sup> Additionally, phosphodiesterases have been shown to limit the spread of cAMP and cGMP in shaping and organizing intracellular signaling microdomains.<sup>64</sup> The striking  $Mn^{2+}$  dependency of formation of cCMP and cUMP by purified sGC provides us with a unique opportunity to assess the possible physiological relevance of  $Mn^{2+}$  in sGC regulation in intact cells. Specifically, if  $Mn^{2+}$  is physiologically relevant for sGC in intact cells, we then expect NO-stimulated formation of cCMP and cUMP to occur. If  $Mg^{2+}$  is physiologically relevant for sGC in intact cells, we then expect no NO-stimulated

formation of cCMP and cUMP to occur. With our newly developed HPLC–MS/MS method, we will address these highly important questions in a forthcoming study. These studies will be fundamentally important for the field of NCs in general because so far, for no enzyme of this class has the question of the physiological relevance of  $Mn^{2+}$  or  $Mg^{2+}$  as a cofactor been resolved. However, striking differential impacts of  $Mg^{2+}$  and  $Mn^{2+}$  have also been observed for the activation and inhibition of mammalian membranous ACs by diterpenes.<sup>65</sup> Also, from the perspective of  $Mn^{2+}$  as an important trace element in the human body,<sup>60,61</sup> the differential regulation of formation of cNMP by sGC provides a unique opportunity to address this as yet poorly understood issue.

**Some Future Studies.** Further studies will have to elucidate if sGC isoform  $\alpha_2\beta_1$ , which is predominately expressed in brain and fetal tissue, also exhibits NC activity. sGC isoforms  $\alpha_1\beta_1$  and  $\alpha_2\beta_1$  contain equivalent amounts of heme, exhibit comparable kinetic properties, and exhibit very similar sensitivity toward NO.<sup>5</sup> As has been observed for the  $\alpha_1\beta_1$  isoform, ODQ inhibited and YC-1 stimulated and sensitized the  $\alpha_2\beta_1$  enzyme toward NO and carbon monoxide.<sup>5</sup> However, binding of NTPs other than GTP and NC kinetic parameters have not yet been assessed for  $\alpha_2\beta_1$ . Future studies also have to investigate the substrate specificity of the membrane-bound GCs (pGCs). Although they are highly homologous in the catalytic domains to sGC,<sup>4</sup> there are some differences to note. pGCs are homodimers and are regulated by peptide and ATP binding. In contrast to sGC, both subunits constitute catalytically active domains that act via positive cooperativity.<sup>66</sup> Particulate fractions from sea urchin sperm and crude membranes obtained from homogenates of rat kidney have already been demonstrated to generate cIMP<sup>16</sup> and cAMP,<sup>20</sup> respectively. However, analysis of a highly purified membrane preparation concerning NC activity is still missing. On the basis of our data for sGC, we predict that pGCs also exhibit substantial NC activities.

Crystallization of holo-sGC is an ambitious goal, and so far, the efforts of several leading laboratories in this field have been unsuccessful. Our results should aid the crystallization of sGC. Previous crystallization experiments may have failed because of a lack of stabilizing ligands. Specifically, the inclusion of MANT- and/or TNP-substituted cytosine, uracil, and/or hypoxanthine nucleotides may facilitate future crystallization efforts. In the case of mACs, MANT- and TNP-nucleotides turned out to be most valuable ligands for crystallography.<sup>67–69</sup> Moreover, MANT- and TNP-nucleotides are the most valuable tools for studying different active mAC conformations.<sup>11</sup> By analogy, the use of fluorescent nucleotides may also facilitate the analysis of the assumed activation-dependent interaction of sGC with various purine and pyrimidine nucleotides.

## ■ ASSOCIATED CONTENT

### ● Supporting Information

Comparison of radiometric and HPLC–MS/MS methods as well as time courses of sGC's NC activity in the presence of  $Mn^{2+}$  and  $Mg^{2+}$  and its inhibition by ATP in the presence of  $Mn^{2+}$  and  $Mg^{2+}$ . This material is available free of charge via the Internet at <http://pubs.acs.org>.

## ■ AUTHOR INFORMATION

### Corresponding Author

\*Institute of Pharmacology, Hannover Medical School, Carl-Neuberg-Str. 1, D-30625 Hannover, Germany. Telephone:



+49-511/532-2805. Fax: +49-511/532-4081. E-mail: seifert.roland@mh-hannover.de.

## Funding

This work was supported by a grant from the Deutsche Forschungsgemeinschaft (Se 529/5-2) to R.S.

## ACKNOWLEDGMENTS

We thank Mrs. Annette Garbe, Mrs. Ingelore Hackbarth, and Mrs. Juliane von der Ohe for expert technical work. Thanks also to the reviewers of this paper for their very constructive critique.

## DEDICATION

This publication is dedicated to Prof. Günter Schultz' 75th anniversary. Günter Schultz is a pioneer in cGMP and sGC research.

## ABBREVIATIONS

AC, adenylyl cyclase; ATP, adenosine 5'-triphosphate; cAMP, adenosine 3',5'-cyclic monophosphate; CC, cytidyl cyclase; cCMP, cytidine 3',5'-cyclic monophosphate; cGMP, guanosine 3',5'-cyclic monophosphate; cIMP, inosine 3',5'-cyclic monophosphate; cNMP, nucleoside 3',5'-cyclic monophosphate; cTMP, thymidine 3',5'-cyclic monophosphate; CTP, cytosine 5'-triphosphate; cUMP, uridine 3',5'-cyclic monophosphate; cXMP, xanthosine 3',5'-cyclic monophosphate; GC, guanylyl cyclase; GTP, guanosine 5'-triphosphate; HPLC-MS/MS, high-performance liquid chromatography and tandem mass spectrometry; IC, inositol cyclase; ITP, inosine 5'-triphosphate; mAC, membranous adenylyl cyclase; MANT-nucleotides, 2'(3')-O-(N-methylanthraniloyl) nucleotides; NC, nucleotidyl cyclase; NO, nitric oxide; NTP, nucleoside 5'-triphosphate; ODQ, [1,2,4]oxadiazolo[4,3-a]quinoxalin-1-one; SEM, standard error of the mean; SNP, sodium nitroprusside; TC, thymidinyl cyclase; TNP-nucleotides, 2',3'-O-(2,4,6-trinitrophenyl) nucleotides; dTTP, thymidine 5'-triphosphate; UC, uridylyl cyclase; UTP, uridine 5'-triphosphate; XC, xanthosinyl cyclase; XTP, xanthosine 5'-triphosphate.

## REFERENCES

- (1) Kots, A. Y., Martin, E., Sharina, I. G., and Murad, F. (2009) A short history of cGMP, guanylyl cyclases, and cGMP-dependent protein kinases. *Handb. Exp. Pharmacol.* 191, 1–14.
- (2) Lucas, K. A., Pitari, G. M., Kazerounian, S., Ruiz-Stewart, I., Park, J., Schulz, S., Chepenik, K. P., and Waldman, S. A. (2000) Guanylyl cyclases and signaling by cyclic GMP. *Pharmacol. Rev.* 52, 375–414.
- (3) Hoffmann, L. S., Schmidt, P. M., Keim, Y., Schaefer, S., Schmidt, H. H. H. W., and Stasch, J. P. (2009) Distinct molecular requirements for activation or stabilization of soluble guanylyl cyclase upon haem oxidation-induced degradation. *Br. J. Pharmacol.* 157, 781–795.
- (4) Derbyshire, E. R., and Marletta, M. A. (2009) Biochemistry of soluble guanylate cyclase. *Handb. Exp. Pharmacol.* 191, 17–31.
- (5) Russwurm, M., Behrends, S., Harteneck, C., and Koesling, D. (1998) Functional properties of a naturally occurring isoform of soluble guanylyl cyclase. *Biochem. J.* 335, 125–130.
- (6) Stasch, J.-P., Pacher, P., and Evgenov, O. V. (2011) Soluble guanylate cyclase as an emerging therapeutic target in cardiopulmonary disease. *Circulation* 123, 2263–2273.
- (7) Garthwaite, J., Southam, E., Boulton, C. L., Nielsen, E. B., Schmidt, K., and Mayer, B. (1995) Potent and selective inhibition of nitric oxide-sensitive guanylyl cyclase by 1H-[1,2,4]oxadiazolo[4,3-a]quinoxalin-1-one. *Mol. Pharmacol.* 48, 184–188.

- (8) Zhao, Y., Brandish, P. E., DiValentin, M., Schelvis, J. P. M., Babcock, G. T., and Marletta, M. A. (2000) Inhibition of soluble guanylate cyclase by ODQ. *Biochemistry* 39, 10848–10854.
- (9) Gille, A., Lushington, G. H., Mou, T.-C., Doughty, M. B., Johnson, R. A., and Seifert, R. (2004) Differential inhibition of adenylyl cyclase isoforms and soluble guanylyl cyclase by purine and pyrimidine nucleotides. *J. Biol. Chem.* 279, 19955–19969.
- (10) Suryanarayana, S., Go, M., Hu, M., Gille, A., Mou, T.-C., Sprang, S. R., Richter, M., and Seifert, R. (2009) Differential inhibition of various adenylyl cyclase isoforms and substituted nucleoside 5'-triphosphates. *J. Pharmacol. Exp. Ther.* 330, 687–695.
- (11) Pinto, C., Lushington, G. H., Richter, M., Gille, A., Geduhn, J., König, B., Mou, T.-C., Sprang, S. R., and Seifert, R. (2011) Structure-activity relationships for the interactions of 2'- and 3'-(O)-(N-methyl)anthraniloyl-substituted purine and pyrimidine nucleotides with mammalian adenylyl cyclases. *Biochem. Pharmacol.* 82, 358–370.
- (12) Hardman, J. G., and Sutherland, E. W. (1969) Guanylyl cyclase, an enzyme catalyzing the formation of guanosine 3',5'-monophosphate from guanosine triphosphate. *J. Biol. Chem.* 244, 6363–6370.
- (13) Zwiller, J., Basset, P., and Mandel, P. (1981) Rat brain guanylate cyclase. Purification, amphiphilic properties and immunological characterization. *Biochim. Biophys. Acta* 658, 64–75.
- (14) Mittal, C. K., Braugher, J. M., Ichihara, K., and Murad, F. (1979) Synthesis of adenosine 3',5'-monophosphate by guanylate cyclase, a new pathway for its formation. *Biochim. Biophys. Acta* 585, 333–342.
- (15) Derbyshire, E. R., Fernhoff, N. B., Deng, S., and Marletta, M. A. (2009) Nucleotide regulation of soluble guanylate cyclase substrate specificity. *Biochemistry* 48, 7519–7524.
- (16) Garbers, D. L., Suddath, J. L., and Hardman, J. G. (1975) Enzymatic formation of inosine 3',5'-monophosphate and of 2'-deoxyguanosine 3',5'-monophosphate. Inosinate and deoxyguanylate cyclase activity. *Biochim. Biophys. Acta* 377, 174–185.
- (17) Gerzer, R., Böhme, E., Hofmann, F., and Schultz, G. (1981) Soluble guanylate cyclase purified from bovine lung contains heme and copper. *FEBS Lett.* 132, 71–74.
- (18) Gerzer, R., Hofmann, F., Böhme, E., Ivanova, K., Spies, C., and Schultz, G. (1981) Purification of soluble guanylate cyclase without loss of stimulation by sodium nitroprusside. *Adv. Cyclic Nucleotide Res.* 14, 255–261.
- (19) Gerzer, R., Hofmann, F., and Schultz, G. (1981) Purification of a soluble, sodium-nitroprusside-stimulated guanylate cyclase from bovine lung. *Eur. J. Biochem.* 116, 479–486.
- (20) Waldman, S. A., Rapoport, R. M., and Murad, F. (1984) Atrial natriuretic factor selectively activates particulate guanylate cyclase and elevates cyclic GMP in rat tissues. *J. Biol. Chem.* 259, 14332–14334.
- (21) Horton, J. K., Martin, R. C., Kalinka, S., Cushing, A., Kitcher, J. P., O'Sullivan, M. J., and Baxendale, P. M. (1992) Enzyme immunoassays for the estimation of adenosine 3',5'-cyclic monophosphate and guanosine 3',5'-cyclic monophosphate in biological fluids. *J. Immunol. Methods* 155, 31–40.
- (22) Werner, K., Schwede, F., Genieser, H.-G., Geiger, J., and Butt, E. (2011) Quantification of cAMP and cGMP analogs in intact cells: Pitfalls in enzyme immunoassays for cyclic nucleotides. *Naunyn-Schmiedeberg's Arch. Pharmacol.* 384, 169–176.
- (23) Hoenicka, M., Becker, E. M., Apeler, H., Sirichoke, T., Schröder, H., Gerzer, R., and Stasch, J. P. (1999) Purified soluble guanylyl cyclase expressed in a baculovirus/Sf9 system: Stimulation by YC-1, nitric oxide, and carbon monoxide. *J. Mol. Med.* 77, 14–23.
- (24) Göttele, M., Dove, S., Kees, F., Schlossmann, J., Geduhn, J., König, B., Shen, Y., Tang, W.-J., Kaever, V., and Seifert, R. (2010) Cytidylyl and uridylyl cyclase activity of *Bacillus anthracis* edema factor and *Bordetella pertussis* CyaA. *Biochemistry* 49, 5494–5503.
- (25) Ruiz-Stewart, I., Tiyyagura, S. R., Lin, J. E., Kazerounian, S., Pitari, G. M., Schulz, S., Martin, E., Murad, F., and Waldman, S. A. (2004) Guanylyl cyclase is an ATP sensor coupling nitric oxide signaling to cell metabolism. *Proc. Natl. Acad. Sci. U.S.A.* 101, 37–42.

- (26) Rauch, A., Leipelt, M., Russwurm, M., and Steegborn, C. (2008) Crystal structure of the guanylyl cyclase Cya2. *Proc. Natl. Acad. Sci. U.S.A.* 105, 15720–15725.
- (27) Winger, J. A., Derbyshire, E. R., Lamers, M. H., Marletta, M. A., and Kuriyan, J. (2008) The crystal structure of the catalytic domain of a eukaryotic guanylate cyclase. *BMC Struct. Biol.* 8, 42.
- (28) Tesmer, J. J., Sunahara, R. K., Johnson, R. A., Gosselin, G., Gilman, A. G., and Sprang, S. R. (1999) Two-metal-ion catalysis in adenylyl cyclase. *Science* 285, 756–760.
- (29) Chang, F.-J., Lemme, S., Sun, Q., Sunahara, R. K., and Beuve, A. (2005) Nitric oxide-dependent allosteric inhibitory role of a second nucleotide binding site in soluble guanylyl cyclase. *J. Biol. Chem.* 280, 11513–11519.
- (30) Emmons, T. L., Mathis, K. J., Shuck, M. E., Reitz, B. A., Curran, D. F., Walker, M. C., Leone, J. W., Day, J. E., Bienkowski, M. J., Fischer, H. D., and Tomasselli, A. G. (2009) Purification and characterization of recombinant human soluble guanylate cyclase produced from baculovirus-infected insect cells. *Protein Expression Purif.* 65, 133–139.
- (31) Schmidt, P., Schramm, M., Schröder, H., and Stasch, J.-P. (2003) Mechanisms of nitric oxide independent activation of soluble guanylyl cyclase. *Eur. J. Pharmacol.* 468, 167–174.
- (32) Mathis, K. J., Emmons, T. L., Curran, D. F., Day, J. E., and Tomasselli, A. G. (2008) High yield purification of soluble guanylate cyclase from bovine lung. *Protein Expression Purif.* 60, 58–63.
- (33) Tomita, T., Tsuyama, S., Imai, Y., and Kitagawa, T. (1997) Purification of bovine soluble guanylate cyclase and ADP-ribosylation on its small subunit by bacterial toxins. *J. Biochem.* 122, 531–536.
- (34) Stone, J. R., and Marletta, M. A. (1995) Heme stoichiometry of heterodimeric soluble guanylate cyclase. *Biochemistry* 34, 14668–14674.
- (35) Humbert, P., Niroomand, F., Fischer, G., Mayer, B., Koesling, D., Hinsch, K. D., Gausepohl, H., Frank, R., Schultz, G., and Böhme, E. (1990) Purification of soluble guanylyl cyclase from bovine lung by a new immunoaffinity chromatographic method. *Eur. J. Biochem.* 190, 273–278.
- (36) Ohlstein, E. H., Wood, K. S., and Ignarro, L. J. (1982) Purification and properties of heme-deficient hepatic soluble guanylate cyclase: Effects of heme and other factors on enzyme activation by NO, NO-heme, and protoporphyrin IX. *Arch. Biochem. Biophys.* 218, 187–198.
- (37) Ignarro, L. J., Degnan, J. N., Baricos, W. H., Kadowitz, P. J., and Wolin, M. S. (1982) Activation of purified guanylate cyclase by nitric oxide requires heme. Comparison of heme-deficient, heme-reconstituted and heme-containing forms of soluble enzyme from bovine lung. *Biochim. Biophys. Acta* 718, 49–59.
- (38) Yazawa, S., Tsuchiya, H., Hori, H., and Makino, R. (2006) Functional characterization of two nucleotide-binding sites in soluble guanylate cyclase. *J. Biol. Chem.* 281, 21763–21770.
- (39) Cech, S. Y., and Ignarro, L. J. (1977) Cytidine 3',5'-monophosphate (cyclic CMP) formation in mammalian tissues. *Science* 198, 1063–1065.
- (40) Gaion, R. M., and Krishna, G. (1979) Cytidylate cyclase: The product isolated by the method of Cech and Ignarro is not cytidine 3',5'-monophosphate. *Biochem. Biophys. Res. Commun.* 86, 105–111.
- (41) Anderson, T. R. (1982) Cyclic cytidine 3',5'-monophosphate (cCMP) in cell regulation. *Mol. Cell. Endocrinol.* 28, 373–385.
- (42) Yamamoto, I., Takai, T., and Mori, S. (1989) Cytidylate cyclase activity in mouse tissues: The enzymatic conversion of cytidine 5'-triphosphate to cytidine 3',5'-cyclic monophosphate (cyclic CMP). *Biochim. Biophys. Acta* 993, 191–198.
- (43) Newton, R. P., Salvage, B. J., and Hakeem, N. A. (1990) Cytidylate cyclase: Development of assay and determination of kinetic properties of a cytidine 3',5'-cyclic monophosphate-synthesizing enzyme. *Biochem. J.* 265, 581–586.
- (44) Muto, N., Kanoh, M., and Yamamoto, I. (1993) Cytidylate cyclase activity is stimulated via activation of a guanine nucleotide-binding protein. *Life Sci.* 52, 13–20.
- (45) Rothkegel, C., Schmidt, P. M., Atkins, D.-J., Hoffmann, L. S., Schmidt, H. H. W., Schröder, H., and Stasch, J.-P. (2007) Dimerization region of soluble guanylate cyclase characterized by bimolecular fluorescence complementation *in vivo*. *Mol. Pharmacol.* 72, 1181–1190.
- (46) Newton, R. P., Salih, S. G., Salvage, B. J., and Kingston, E. E. (1984) Extraction, purification and identification of cytidine 3',5'-cyclic monophosphate from rat tissues. *Biochem. J.* 221, 665–673.
- (47) Newton, R. P., Kingston, E. E., Hakeem, N. A., Salih, S. G., Beynon, J. H., and Moyse, C. D. (1986) Extraction, purification, identification and metabolism of 3',5'-cyclic UMP, 3',5'-cyclic IMP and 3',5'-cyclic dTMP from rat tissues. *Biochem. J.* 236, 431–439.
- (48) Ervens, J., and Seifert, R. (1991) Differential modulation by N<sup>4</sup>,2'-O-dibutyl cytidine 3',5'-cyclic monophosphate of neutrophil activation. *Biochem. Biophys. Res. Commun.* 174, 258–267.
- (49) Desch, M., Schinner, E., Kees, F., Hofmann, F., Seifert, R., and Schlossmann, J. (2010) Cyclic cytidine 3',5'-monophosphate (cCMP) signals via cGMP kinase I. *FEBS Lett.* 584, 3979–3984.
- (50) Reinecke, D., Burhenne, H., Sandner, P., Kaever, V., and Seifert, R. (2011) Human cyclic nucleotide phosphodiesterases possess a much broader substrate-specificity than previously appreciated. *FEBS Lett.* 585, 3259–3262.
- (51) Wolter, S., Golombek, M., and Seifert, R. (2011) Differential activation of cAMP- and cGMP-dependent protein kinases by cyclic purine and pyrimidine nucleotides. *Biochem. Biophys. Res. Commun.* 415, 563–566.
- (52) Vila-Petroff, M. G., Younes, A., Egan, J., Lakatta, E. G., and Sollott, S. J. (1999) Activation of distinct cAMP-dependent and cGMP-dependent pathways by nitric oxide in cardiac myocytes. *Circ. Res.* 84, 1020–1031.
- (53) Wörner, R., Lukowski, R., Hofmann, F., and Wegener, J. W. (2007) cGMP signals mainly through cAMP kinase in permeabilized murine aorta. *Am. J. Physiol.* 292, H237–H244.
- (54) Ciani, E., Guidi, S., Della Valle, G., Perini, G., Bartesaghi, R., and Contestabile, A. (2002) Nitric oxide protects neuroblastoma cells from apoptosis induced by serum deprivation through cAMP-response element-binding protein (CREB) activation. *J. Biol. Chem.* 277, 49896–49902.
- (55) Xu, H.-L., Wolde, H. M., Gavriluk, V., Baughman, V. L., and Pelligrino, D. A. (2004) cAMP modulates cGMP-mediated cerebral arteriolar relaxation *in vivo*. *Am. J. Physiol.* 287, H2501–H2509.
- (56) Voth, D. E., Hamm, E. E., Nguyen, L. G., Tucker, A. E., Salles, I. I., Ortiz-Leduc, W., and Ballard, J. D. (2005) *Bacillus anthracis* oedema toxin as a cause of tissue necrosis and cell type-specific cytotoxicity. *Cell. Microbiol.* 7, 1139–1149.
- (57) Jitrapakdee, S., St Maurice, M., Rayment, I., Cleland, W. W., Wallace, J. C., and Attwood, P. V. (2008) Structure, mechanism and regulation of pyruvate carboxylase. *Biochem. J.* 413, 369–387.
- (58) Kim, K. H., Rodriguez, A. M., Carrico, P. M., and Melendez, J. A. (2001) Potential mechanisms for the inhibition of tumor cell growth by manganese superoxide dismutase. *Antioxid. Redox Signaling* 3, 361–373.
- (59) Barceloux, D. G. (1999) Manganese. *J. Toxicol. Clin. Toxicol.* 37, 293–307.
- (60) Rucker, D., Thadhani, R., and Tonelli, M. (2010) Trace element status in hemodialysis patients. *Semin. Dial.* 23, 389–395.
- (61) Wood, R. J. (2009) Manganese and birth outcome. *Nutr. Rev.* 67, 416–420.
- (62) Bidmon, H.-J., Mohlberg, H., Habermann, G., Buse, E., Zilles, K., and Behrends, S. (2006) Cerebellar localization of the NO-receptive soluble guanylyl cyclase subunits- $\alpha 2/\beta 1$  in non-human primates. *Cell Tissue Res.* 326, 707–714.
- (63) Tresguerres, M., Levin, L. R., and Buck, J. (2011) Intracellular cAMP signaling by soluble adenylyl cyclase. *Kidney Int.* 79, 1277–1288.
- (64) Fischmeister, R., Castro, L. R. V., Abi-Gerges, A., Rochais, F., Jurevicius, J., Leroy, J., and Vandecasteele, G. (2006) Compartmentation of cyclic nucleotide signaling in the heart: The role of cyclic nucleotide phosphodiesterases. *Circ. Res.* 99, 816–828.

- (65) Erdorf, M., Mou, T.-C., and Seifert, R. (2011) Impact of divalent metal ions on regulation of adenylyl cyclase isoforms by forskolin analogs. *Biochem. Pharmacol.* 82, 1673–1681.
- (66) Joubert, S., McNicoll, N., and De Léan, A. (2007) Biochemical and pharmacological characterization of P-site inhibitors on homodimeric guanylyl cyclase domain from natriuretic peptide receptor-A. *Biochem. Pharmacol.* 73, 954–963.
- (67) Mou, T.-C., Gille, A., Suryanarayana, S., Richter, M., Seifert, R., and Sprang, S. R. (2006) Broad specificity of mammalian adenylyl cyclase for interaction with 2',3'-substituted purine and pyrimidine nucleotide inhibitors. *Mol. Pharmacol.* 70, 878–886.
- (68) Mou, T.-C., Gille, A., Fancy, D. A., Seifert, R., and Sprang, S. R. (2005) Structural basis for the inhibition of mammalian membrane adenylyl cyclase by 2'(3')-O-(N-methylanthraniloyl)-guanosine 5'-triphosphate. *J. Biol. Chem.* 280, 7253–7261.
- (69) Hübner, M., Dixit, A., Mou, T.-C., Lushington, G. H., Pinto, C., Gille, A., Geduhn, J., König, B., Sprang, S. R., and Seifert, R. (2011) Structural basis for the high-affinity inhibition of mammalian membranous adenylyl cyclase by 2',3'-O-(N-methylanthraniloyl)-inosine 5'-triphosphate. *Mol. Pharmacol.* 80, 87–96.